

Numerical Simulations of the Light Propagation in the Gravitational Field of Moving Bodies

Sergei A. Klioner and Michael Peip

Lohrmann Observatory, Dresden Technical University, Mommsenstr. 13, 01062 Dresden,
Germany

Received December 17, 2018/ Accepted December 17, 2018

Abstract. One of the most subtle points in the current relativistic models for microarc-second astrometrical observations is the treatment of the influence of translational motion of gravitating bodies on the light propagation. This paper describes numerical simulations of the light propagation in the gravitational field of moving gravitating bodies as well as summarizes the underlying theory. The simulations include high-precision numerical integrations of both post-Newtonian and post-Minkowskian differential equations of light propagation and a detailed comparison of the results of the numerical integrations with various available approximate analytical formulas. The simulations has been performed both for hypothetical bodies with various parameters of trajectories as well as for all the major bodies of the solar system using the JPL ephemeris DE405/LE405 to calculate their motion.

It is shown that for the accuracy of $\sim 0.2 \mu\text{as}$ it is sufficient to use the well-known solution for the light propagation in the field of a motionless mass monopole and substitute in that solution the position of the body at the moment of closest approach between the actual trajectory of the body and the unperturbed light path (as it was first suggested by Hellings (1986)). For a higher accuracy one should use either the post-Newtonian solution for uniformly moving bodies (Klioner & Kopeikin 1992) or the post-Minkowskian solution for arbitrarily moving bodies (Kopeikin & Schäfer 1999). For astrometric observations performed from within the solar system these two solutions guarantee the accuracy of $\sim 0.002 \mu\text{as}$ and are virtually indistinguishable from each other.

Key words. astrometry – reference systems – relativity – gravitational lensing

1. Introduction

It is widely known that extremely high accuracy of the future space-born astrometric missions like GAIA (ESA 2000; Perryman et al. 2001; Bienaymé & Turon 2002) and SIM

Send offprint requests to: Sergei A. Klioner, e-mail: klioner@rcs.urz.tu-dresden.de

(Shao 1998) makes it necessary to formulate the reduction model of positional observations in a form fully consistent with General Relativity Theory (GRT). The relativistic models of positional observations has been formulated by several groups of authors: Klioner (1989), Brumberg, Klioner, & Kopejkin (1990), Klioner & Kopeikin (1992), de Felice et al. (1998), de Felice et al. (2000), de Felice et al. (2001), Klioner (2003a). This paper is devoted to an investigation of one subtle point in any microarcsecond relativistic model of positional observations. Namely, the influence of the translational motion of gravitating bodies on the light propagation is investigated here in great detail.

After the pioneering work of Hellings (1986) where it was suggested to compute the positions of the gravitating bodies at the moment of closest approach between the body and the unperturbed light ray and substitute these positions into the well-known solution for the light propagation in the gravitational field of a system of motionless bodies, several authors has succeeded to formulate more rigorous approaches to the problem (Klioner 1989, 1991; Klioner & Kopeikin 1992; Kopeikin & Schäfer 1999; Kopeikin & Mashhoon 2002). Detailed historical overviews can be found in Introduction of Kopeikin & Schäfer (1999) and in Section 6 of Klioner (2003a) (see also Klioner (2003b)).

In this paper we perform extensive numerical simulations aimed at clarifying the ability of various approximate analytical formulas to reproduce the gravitational light deflection in the field of the solar system at the level of $0.1 - 1 \mu\text{as}$ as required by GAIA and SIM.

Possible ways to compute the light trajectory in the gravitational field of moving bodies are summarized in Section 2. Section 3 explains general layout of the simulations. The results of the simulations are discussed in Section 4. The suggestions for practical relativistic modeling of high-accuracy positional observations depending on the goal accuracy are formulated in Section 5. In the Appendices we summarize the theoretical formulas concerning the influence of the translational motion of the gravitating bodies on the light propagation. Most of these formulas are used in the simulations. Appendix A contains general formulas for null geodesics in the weak-field approximation. Both post-Newtonian and post-Minkowskian equations are given there. The most important theoretical results for the light propagation in the post-Newtonian approximation are given in Appendix B. The equations of light propagation in the post-Minkowskian approximation are discussed in Appendix C. The two point boundary problem for the analytical solutions is discussed in Appendix D.

2. Possible ways to calculate the light propagation in the field of moving bodies

According to the theory described in the Appendices there are several ways to calculate the light trajectory in the gravitational field of moving mass monopoles:

1. Numerical integration of the post-Minkowskian differential equations of light propagation (C.11)–(C.22) with initial conditions (C.25)–(C.27).

2. Analytical post-Minkowskian solution (C.28)–(C.33) for arbitrarily moving bodies (the solution for the position of the photon (C.28) contains an integral that can be computed numerically, or estimated to be negligible for a particular purpose and thus neglected).
3. Numerical integration of the post-Newtonian equations of light propagation (B.5)–(B.12) with initial conditions (B.13)–(B.14).
4. Analytical post-Newtonian solution for uniformly moving mass monopoles (B.15)–(B.26) with two free parameters \mathbf{x}_{A0} and \mathbf{v}_A to be related to the actual trajectory of the body.

As discussed in the Appendices below the post-Minkowskian approximation scheme deals with expansions in powers of the gravitational constant G . The first post-Minkowskian approximation implies that all terms of order $\mathcal{O}(G^2)$ are neglected. The post-Newtonian approximation scheme operates with expansions in powers of c^{-1} . In the first post-Newtonian approximation terms of order $\mathcal{O}(c^{-4})$ are neglected in the equations of light propagation. One can prove that in the case of light propagation the formulas of the first post-Newtonian approximation are linear in G and, therefore, contained in those of the first post-Minkowskian approximation.

The most accurate way to calculate the light propagation is clearly the first one, i.e. numerical integration of the post-Minkowskian differential equations of motion for the photon. The errors of those differential equations of motion comes from the effects of the second post-Minkowskian (or post-Newtonian) approximation which are known to be negligible for the solar system applications. Numerical integration of the post-Newtonian equations of motion for the photon (B.5)–(B.12) can also be used to calculate the light trajectory in the field of arbitrarily moving bodies. However, since the post-Newtonian equations of motion are contained in the post-Minkowskian equations of motion (see Appendix C), the former can be used for an internal consistency check of the whole calculation rather than for an independent computation of the light path. Our numerical experiments show that for the solar system applications the results of the numerical integrations of the post-Newtonian and post-Minkowskian equations of motion are identical within the errors of the first post-Minkowskian approximation.

The analytical post-Minkowskian solution given in Appendix C.4 is surely the most accurate analytical solution for the problem. However, (1) the solution for the position of the photon involves an integral which should be in principle computed numerically, and (2) the post-Minkowskian solution is relatively expensive as far as the computing time is concerned since it contains the retarded moment of time to be computed by iterations (see below). On the other hand, the full accuracy of the analytical post-Minkowskian solution is not necessary to attain the accuracy of 1 μ as for the solar system applications. More simple analytical solutions of sufficient accuracy can be found instead.

The fully analytical post-Newtonian solution given in Appendix B.4 describes the light trajectory in the field of uniformly moving gravitating bodies having the coordinates

$$\mathbf{x}_A(t) = \mathbf{x}_{A0} + \mathbf{v}_A(t - t_0), \quad (1)$$

where \mathbf{x}_{A0} and \mathbf{v}_A are two arbitrary constant vectors. These constants can be related to the actual trajectory of the body $\mathbf{x}_A^{\text{eph}}(t)$ in different ways with the hope that the errors related to the non-uniformity of the body's trajectory will be minimized in some sense. The principal goal of this paper is to check if the analytical post-Newtonian solution with some reasonable choice of the constants \mathbf{x}_{A0} and \mathbf{v}_A characterizing the trajectory of the body can describe the gravitational light deflection with an accuracy of $0.1 - 1 \mu\text{as}$.

For the analytical post-Newtonian solution one has to choose either a fixed point or a straight line as the model trajectory $\mathbf{x}_A(t)$ of the body. In this paper we consider six choices for the constants \mathbf{x}_{A0} and \mathbf{v}_A in the post-Newtonian solution: four solutions for a body at rest named P_1 , P_2 , P_3 and P'_3 and two solutions for a body moving with constant velocity L_1 and L_2 (see Figure 1). Each of the considered solutions uses the actual position (and possibly velocity) of the body at some reference moment of time $t = t_{\text{ref}}$. The most simple solution P_1 uses the fixed position $\mathbf{x}_A^{\text{eph}}(t_o)$ of the body at the moment of observation $t_{\text{ref}} = t_o$. The fixed position $\mathbf{x}_A^{\text{eph}}(t^{\text{ca}})$ of the body at the moment $t_{\text{ref}} = t^{\text{ca}}$ of closest approach between the body and the unperturbed light path is used for the second solution P_2 . The moment t^{ca} can be calculated as

$$t^{\text{ca}} = \max \left(t_e, t_o - \max \left(0, \frac{\mathbf{g} \cdot (\mathbf{x}_o(t_o) - \mathbf{x}_A^{\text{eph}}(t_o))}{c |\mathbf{g}|^2} \right) \right), \quad (2)$$

$$\mathbf{g} = \mu - \frac{1}{c} \dot{\mathbf{x}}_A^{\text{eph}}(t_o), \quad (3)$$

where t_e is the moment of emission of the photon. If the source is situated outside of the solar system one can put $t_e = -\infty$ and the outer max can be omitted in (2). The retarded moment of time t^* is used as t_{ref} in the solution P_3 . This moment of time is defined by

$$t^* + \frac{1}{c} |\mathbf{x}_p(t) - \mathbf{x}_A^{\text{eph}}(t^*)| = t. \quad (4)$$

The moment t^* is relatively expensive to calculate since the equation (4) is an implicit one and one has to use some kind of iterations to solve it (e.g., Newton's method). That is why, one can try to substitute t^* by its simplified version t^{**} which can be directly calculated

$$t^{**} = t - \frac{1}{c} |\mathbf{x}_p(t) - \mathbf{x}_A^{\text{eph}}(t)|. \quad (5)$$

The solution P'_3 uses the position $\mathbf{x}_A^{\text{eph}}(t^{**})$ of the body at $t_{\text{ref}} = t^{**}$.

The solutions L_1 and L_2 are the solutions for a body moving with a constant velocity. In these two cases the parameters \mathbf{x}_{A0} and \mathbf{v}_A of (B.15)–(B.26) are chosen to coincide with the actual position and velocity of the body at the moments $t_{\text{ref}} = t_o$ and $t_{\text{ref}} = t^{\text{ca}}$, respectively (therefore, the trajectories of the bodies used in L_1 and L_2 are tangents to the actual trajectory of the body at these two moments of time). The choice of the trajectories $\mathbf{x}_A(t)$ are summarized in Table 1 and Figure 1.

solution	t_{ref}	\mathbf{x}_{A0}	\mathbf{v}_A
P_1	t_o	$\mathbf{x}_A^{\text{eph}}(t_o)$	0
P_2	t^{ca}	$\mathbf{x}_A^{\text{eph}}(t^{\text{ca}})$	0
P_3	t^*	$\mathbf{x}_A^{\text{eph}}(t^*)$	0
P'_3	t^{**}	$\mathbf{x}_A^{\text{eph}}(t^{**})$	0
L_1	t_o	$\mathbf{x}_A^{\text{eph}}(t_o)$	$\dot{\mathbf{x}}_A^{\text{eph}}(t_o)$
L_2	t^{ca}	$\mathbf{x}_A^{\text{eph}}(t^{\text{ca}})$	$\dot{\mathbf{x}}_A^{\text{eph}}(t^{\text{ca}})$

Table 1. Choice of the constants for the six analytical post-Newtonian solutions for the light trajectory considered in the present paper (see text for further explanations).

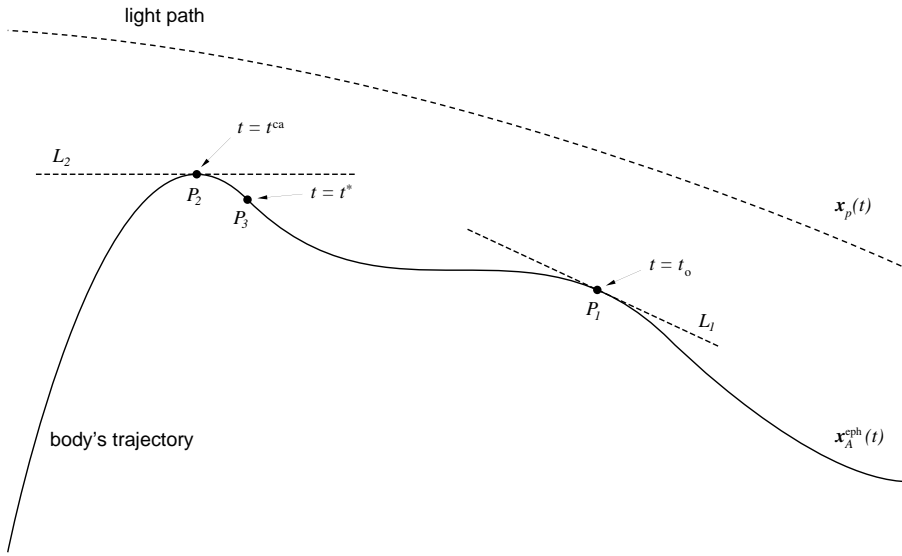


Fig. 1. Actual trajectory $\mathbf{x}_A^{\text{eph}}(t)$ of body A and the five simplified trajectories used to model the light propagation within the post-Newtonian approximation scheme: three fixed positions P_1 ($\mathbf{x}_A(t) = \mathbf{x}_A^{\text{eph}}(t_o) = \text{const}$), P_2 ($\mathbf{x}_A(t) = \mathbf{x}_A^{\text{eph}}(t^{\text{ca}}) = \text{const}$) and P_3 ($\mathbf{x}_A(t) = \mathbf{x}_A^{\text{eph}}(t^*) = \text{const}$), and two trajectories with constant velocity L_1 ($\mathbf{x}_A(t) = \mathbf{x}_A^{\text{eph}}(t_o) + \dot{\mathbf{x}}_A^{\text{eph}}(t_o)(t - t_o)$) and L_2 ($\mathbf{x}_A(t) = \mathbf{x}_A^{\text{eph}}(t^{\text{ca}}) + \dot{\mathbf{x}}_A^{\text{eph}}(t^{\text{ca}})(t - t^{\text{ca}})$). The position P'_3 mentioned in the text is not shown on the sketch. It is situated on the actual trajectory of the body close to P_3 .

3. Simulations

It is clear that numerical integration of the differential equations of light propagation can be performed only for sources situated at some finite distance from the gravitating body (the end point of numerical integrations is anyway at some finite distance since it is defined by the position of observer). Light propagation from a source at a finite distance to the observer represents a two point boundary problem for the differential equations of light propagation. As discussed by Klioner (2003a) the goal of the relativistic reduction of observations in this case is to relate the unit direction \mathbf{n} of the light propagation at the moment of observation to the unit direction \mathbf{k} from the point of light emission $\mathbf{x}(t_0)$ to the point of light observation $\mathbf{x}(t)$ (see, Figure 2).

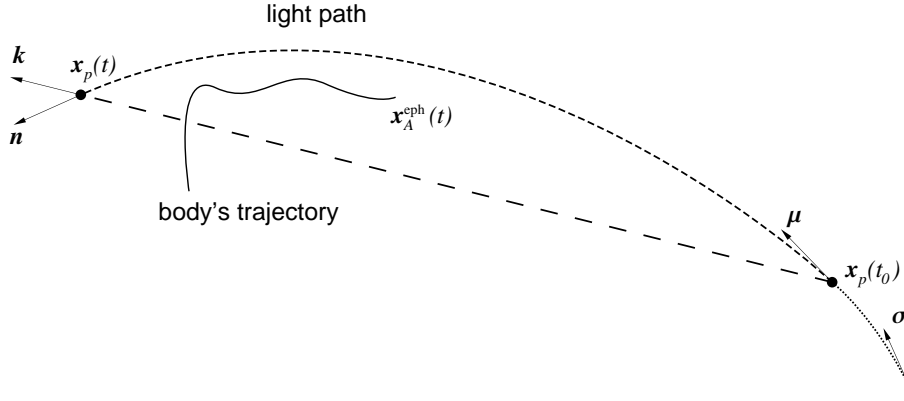


Fig. 2. Four vectors appearing in the calculations: vector μ is the unit light direction at the point of emission $x(t_0)$, n is the light direction at the point of observation $x(t)$, k is the unit coordinate direction from $x(t_0)$ to $x(t)$, and σ is the unit direction of the light propagation for $t \rightarrow -\infty$. Formal definitions of these vectors are given in Appendix D.

In each individual simulation we fix the points of emission and observation for all the solutions. These points are computed by numerical integration of the post-Minkowskian differential equations, so that for this most accurate solution we compute vectors n , μ , $x(t_0)$, $x(t)$ and k with the maximal possible accuracy. Using the formulas given in Appendix D we then solve the two point boundary problem for all the analytical solutions discussed in our simulations and compare the vector n from the post-Minkowskian numerical integration to the vectors n from the analytical solutions. We choose the distance between the point of emission and the gravitating body sufficiently large so that the differences between the vectors n do not change (within an accuracy of 0.001 μ as) when we further increase the distance. Therefore, we can claim that our results are valid also for sources at infinity. Moreover, the simulations have shown that the differences between vectors n for the points of emission at lower distances are smaller than those for sources at infinity. This means that the maximal errors given below are valid also for sources situated at finite distances from the observer (e.g. for the solar system objects).

In order to test the analytical formulas in different situations and check internal consistency of the simulations we have done three independent series of simulations with different choices for the trajectories $x_A^{\text{eph}}(t)$ of the bodies. For all the simulations the masses of the gravitating bodies have been taken from the JPL ephemeris DE405/LE405 while the radii and other parameters of the bodies were taken from Weissman, McFadden & Johnson (1999). The three series of simulations can be described as follows.

A. Parabolic trajectories with constant acceleration (Table 2). For each trajectory the velocity and the acceleration of the body at the moment of closest approach between the body and the photon coincide with the maximal possible barycentric velocity and acceleration of the corresponding body of the solar system. The impact parameter for each trajectory is chosen so that at the moment of closest approach the distance between the photon and the body is equal to the ra-

dius of the corresponding body (expect for the three lines in Table 2 with fixed minimal allowed angular distance ψ_{\min} between the gravitating body and the direction of light propagation as seen by the observer; the minimal avoidance angle for each of these three bodies (Earth, Sun and Moon) are calculated from the condition that the minimal Sun avoidance angle is $\psi_{\min}^{\odot} = 35^{\circ}$). The distance between the observer (satellite) and the gravitating body is taken to be the maximal possible distance between the GAIA satellite and the corresponding body of the solar system (some of the effects under study become larger with increasing this distance and it is important to use the maximal possible distance for the simulations). For the calculation of that maximal distance the satellite were supposed to be situated exactly at the Lagrange point L_2 of the Earth-Sun system. After fixing all these parameters the initial conditions of the photon trajectory are still not unique and this freedom can be used to check all possible mutual orientations of the velocity vector of the photon and the velocity and acceleration vectors of the body at the moment of closest approach. The directions of all these three vectors are independent of each other. Routinely, in a coordinate system where the direction of the velocity of the photon is fixed we check 50 uniformly distributed directions for each of the two other vectors to find the maximal value of the effects under investigation. In several cases we have checked that a finer grid of mutual orientations does not lead to any changes in the maximal differences between the models given in Table 2.

B. Circular coplanar trajectories (Table 3). The observer is supposed to be situated exactly at the Lagrange point L_2 of the Earth-Sun system. Each gravitating body moves along a circular orbit with realistic semi-major axis and mean motion. All the orbits are coplanar. All possible configurations of the observer and the gravitating body have been checked with a step of 0.01 of the siderial period of the corresponding body. The impact parameter of the light ray (i.e. the minimal distance between the photon and the body) is chosen to be not smaller than the radius of the body, but can be larger to meet the requirement imposed by the minimal Sun avoidance angle ψ_{\min}^{\odot} . For all the bodies for which the minimal Sun avoidance angle influence their observability (Sun, Mercury, Venus, Earth and Moon), the simulations has been done with and without taking the minimal Sun avoidance angle of $\psi_{\min}^{\odot} = 35^{\circ}$ into account. For each mutual configuration of the body and the observer 36 different initial positions and velocities of the photon have been chosen so that in the view plane of the observer the observed directions of the light are uniformly distributed around the observed position of the gravitating body. Table 3 contains maximal differences between the models for all the light trajectories investigated for each of the body.

C. Realistic trajectories on the basis of the JPL ephemeris DE405 (Table 4). Simulations similar to **B** have been performed using the JPL numerical ephemeris DE405/LE405 for the trajectories of the gravitating bodies. The orbit of the observer is taken to be a realistic Lissajous-type orbit about the L_2 point of the Earth-Sun system and were computed using the algorithm suggested by Mignard (2002). For each body the minimal Sun avoidance angle of 35° has been

taken into account while choosing the parameters of the light rays. All mutual configurations of the observer and the gravitating bodies between 1 January 2008 and 31 December 2020 have been checked with a step of 1 day (the total time span covers 4749 days). The impact parameters of the light rays are taken in the same way as for simulation **B**. Also in the same way as in simulation **B** we have checked 36 different directions of the light ray uniformly distributed relative to the line connecting the observer and the gravitating body. We also checked in several cases that increasing the number of the observed light directions from 36 to, say, 360, does not change the maximal differences between the models given in Table 3.

For simulations **A**, **B** and **C** an ANSI C program has been written. Since the effects we are looking for can be as small as $10^{-3} \mu\text{as} \approx 5 \cdot 10^{-15}$, it is not sufficient to perform the computations using standard "double" 64-bit arithmetic which provides only 16 decimal digits. Routinely, we have used 80-bit arithmetic on an Intel processor (18 decimal digits). Some additional accuracy checks have been performed using 128-bit arithmetic on an Ultra-Sparc processor (34 decimal digits) and have shown that the 80-bit arithmetic does not produce substantial roundoff errors and is sufficient for our purposes. Note that since the simulations took several weeks of computing time on a Pentium III processor running at 600 MHz (about one million photon trajectories for each gravitating body were checked), it was hardly possible to perform the simulations within a reasonable time using a software environment emulating arithmetic with arbitrary precision (Maple, Mathematica, etc.).

For the numerical integrations of both the post-Minkowskian and post-Newtonian differential equations of motion we have used the Everhart integrator described, e.g. in Everhart (1974, 1985). In our program the Everhart integrators of the orders 7, 11, 13, 15, 19, 23 and 27 are implemented, and the internal coefficients of the integrator are coded with an accuracy consistent with the 128-bit arithmetic. This makes it possible to perform the numerical integration with very high precision (at least, up to 34 decimal digits) in a quite efficient way. Our investigation showed that the number of internal iterations within the integrator can be chosen to be as low as 1 (or at most 2) without any loss of the resulting accuracy. This can be understood as a consequence of almost straight trajectories of the light. The integrator of order 19 was found to be the most efficient for our calculations. The final global accuracy of the numerical integrations was controlled by integrating the solution backwards. The integration is repeated automatically with higher accuracy parameters of the integrator until the required goal accuracy is reached.

The most time-consuming part of the calculations is the numerical integration of the post-Minkowskian differential equations of light propagation given in Appendix C.2). In order to maximally speed up the numerical integration the code calculating the right-hand side of (C.11) has been optimized using the Maple package CODEGEN Char et al. (1993). This optimization reduced the number of necessary float-point operations roughly by a factor of 2.

4. Results of the simulations

The maximal differences between the vectors \mathbf{n} from the numerical post-Minkowskian solution and the various analytical solutions are summarized in Tables 2–4. The following conclusions from the numerical simulations can be formulated:

1. The results of the three independent simulations are in good agreement with each other. This serves as an internal consistency check of the simulations.
2. The post-Minkowskian analytical model is virtually indistinguishable from the numerical integration of the post-Minkowskian differential equations of light propagation and leads to errors of order $0.002 \mu\text{as}$.
3. As expected the naive model for the light propagation involving the post-Newtonian analytical solution for the body being at rest at its position at the moment of observation (the model P_1) is too inaccurate and leads to errors exceeding 1 mas. Note that our software code for the model P_1 does not check if the formally calculated impact parameter of the light rays exceeds the radius of the body (such a check is, of course, easy to implement, but if the software detects that the formal impact parameter is smaller than the radius of the body, this can serve only as an evidence of the inaccuracy of the model P_1 and the situation cannot be corrected within the model P_1). This is the reason why the errors for the model P_1 given in Tables 2–4 sometimes exceed the maximal possible gravitational light deflection due to the corresponding body.
4. The post-Newtonian analytical solution for the body being at rest at its position at the moment of closest approach (P_2) or at the retarded moment of time (P_3) are virtually indistinguishable from each other for the solar system applications (e.g., for Jupiter the maximal difference of these models does not exceed $7.5 \times 10^{-4} \mu\text{as}$).
5. Any of these two models (P_2 and P_3) allows one to attain an accuracy of $\sim 0.18 \mu\text{as}$ for the realistic trajectories of the gravitating bodies (Table 4). The errors of $\sim 0.75 \mu\text{as}$ appearing in the simulation with parabolic trajectories also follow from a simplified analytical considerations and are quoted e.g. in Table 1 of Klioner (2003a) as upper estimates of the effects. The reason for the discrepancy between these estimates for the parabolic trajectories and for the realistic trajectories were already discussed by Klioner (2003a, p. 1590, above Eq. (34)) where the realistic values for Jupiter and Saturn were predicted. One can see that the predicted realistic values and the values from Table 4 are in good agreement.
6. Simplified calculation of the retarded moment of time as given by (5) (model P'_3) increases the errors in the light deflection. The errors attains $\sim 0.3 \mu\text{as}$ for the realistic trajectories of the gravitating bodies.
7. The post-Newtonian analytical model for a body moving with a constant velocity is indistinguishable from the post-Minkowskian model within the accuracy of $0.002 \mu\text{as}$ provided that the position and velocity of the body on the rectilinear model trajectory of the body coincide

with the actual positions and velocities of the body at the moment of the closest approach (model L_2).

8. If the position and velocity of the body on the rectilinear trajectory coincide with the actual positions and velocities at the moment of observation (model L_1) the error exceeds $0.1 \mu\text{as}$.

5. Concluding remarks

The results of our numerical simulations are in good agreement with the theoretical discussion by Klioner (2003a). These results allows one to formulate the following practical recommendations for data processing of microarcsecond positional observations performed from the solar system:

- If an accuracy of $0.2 \mu\text{as}$ is sufficient one can employ the simple post-Newtonian analytical model for the light propagation in the gravitational field of a motionless body and substitute in that model the actual position of the body evaluated either at the moment of closest approach t^{ca} or at the retarded moment t^* . If t^* is used it is necessary to perform at least two iterations to solve the implicit equation (4) for the retarded moment.
- If an accuracy below $0.2 \mu\text{as}$ is required one should use either the full post-Minkowskian analytical model as given in Appendix C.4 (neglecting the integral $g(t_0, t)$ in (C.30)) or the post-Newtonian analytical model for a body moving with a constant velocity (Appendix B.4) and choose the constants \mathbf{x}_{A0} and \mathbf{v}_A of that model to coincide with the actual position and velocity of the body at t^{ca} .

Appendix A: Equations of null geodesics

Here we summarize the formulas for the null geodesics in a weak gravitational field used in this paper. The metric tensor $g_{\alpha\beta}$ is supposed to have the form

$$g_{\alpha\beta} = \eta_{\alpha\beta} + h_{\alpha\beta}, \quad (\text{A.1})$$

where

$$\eta_{\alpha\beta} = \text{diag}(-1, +1, +1, +1) \quad (\text{A.2})$$

is the flat Minkowski metric and $h_{\alpha\beta} = h_{\alpha\beta}(t, \mathbf{x})$ is the non-Galilean part of the metric.

A.1. Post-Newtonian approximation

First, we use the standard post-Newtonian assumptions on the orders of magnitude of $h_{\alpha\beta}$ with respect to the formal parameter c^{-1} :

$$\begin{aligned} h_{00} &= O(c^{-2}), \\ h_{0i} &= O(c^{-3}), \\ h_{ij} &= O(c^{-2}). \end{aligned} \quad (\text{A.3})$$

body	δ	δ^2	pM	pN, P_1	pN, P_2	pN, P_3	pN, P'_3	pN, L_1	pN, L_2
Sun*	$1.76 \cdot 10^6$	15.0	17.7	43.3	17.8	17.8	17.8	17.7	17.7
Sun, $\psi_{\min}^\odot = 35^\circ$	13600	0.001	0.001	0.003	0.002	0.002	0.002	0.001	0.001
Mercury*	82.9	0.0	0.0	93.2	0.016	0.016	0.154	0.601	0.0
Venus	493	0.0	0.0	812	0.058	0.058	0.178	0.357	0.0
Earth*	574	0.0	0.0	8.08	0.058	0.058	0.058	0.0	0.0
Earth, $\psi_{\min}^\odot = 35^\circ$	3.64	0.0	0.0	0.001	0.001	0.001	0.001	0.0	0.0
Moon*	25.9	0.0	0.0	1.44	0.003	0.003	0.003	0.0	0.0
Moon, $\psi_{\min}^\odot = 19^\circ$	0.086	0.0	0.0	0.0	0.0	0.0	0.0	0.0	0.0
Mars	116	0.0	0.0	143	0.010	0.010	0.058	0.096	0.0
Jupiter	16300	0.001	0.002	26900	0.746	0.746	0.847	0.292	0.002
Saturn	5780	0.0	0.0	86100	0.196	0.196	0.250	0.036	0.0
Uranus	2530	0.0	0.0	5960	0.047	0.047	0.110	0.085	0.0
Neptune	2080	0.0	0.0	6530	0.050	0.050	0.106	0.081	0.0

Table 2. The result of simulations using parabolic trajectories $x_A^{\text{eph}}(t)$. All quantities are given in μas . The second column δ is the maximal light deflection angle for the body computed with the post-Minkowskian differential equations of light propagation, while δ^2 is the approximate value of the post-post-Minkowskian terms which are neglected in our considerations. The maximal errors of the post-Minkowskian analytical solution (pM) and the six post-Newtonian solutions (pN) are given. The meaning of P_i and L_i is discussed in Section 2 and summarized in Table 1. The number "0.0" means that the actual value of the effect is less than $0.001 \mu\text{as}$. The bodies designated with a star, e.g. "Mercury**", cannot be observed by GAIA because of the minimal Sun avoidance angle of 35° . The minimal impact angle ψ_{\min} for the Sun and the Earth coincide with the minimal Sun avoidance angle of $\psi_{\min}^\odot = 35^\circ$, while that for the Moon is approximately calculated from simplified orbits of GAIA and the Moon.

Then the equations of null geodesics in the first post-Newtonian approximation read

$$\begin{aligned} \ddot{x}^i = & \frac{1}{2} c^2 h_{00,i} - h_{00,k} \dot{x}^k \dot{x}^i - \left(h_{ik,l} - \frac{1}{2} h_{kl,i} \right) \dot{x}^k \dot{x}^l - \frac{1}{2} h_{00,t} \dot{x}^i \\ & - \left(\frac{1}{c} h_{0k,j} - \frac{1}{2c^2} h_{jk,t} \right) \dot{x}^j \dot{x}^k \dot{x}^i - c (h_{0i,k} - h_{0k,i}) \dot{x}^k \\ & - h_{ik,t} \dot{x}^k + O(c^{-2}), \end{aligned} \quad (\text{A.4})$$

where for any small latin index i except for t one has $A_{,i} = \frac{\partial}{\partial x^i} A$ and $A_{,t} = \frac{\partial}{\partial t} A$. Note that the velocity of the photon $\dot{x}^k = O(c)$. Eq. (A.4) is valid in the post-Newtonian approximation which is also called weak-field-slow-motion approximation. The assumption $h_{0i} = O(c^{-3})$ means that the velocity of the gravitating bodies are considered to be small with respect to c . Therefore, these equations cannot be used if the velocities of the gravitating bodies are large.

body	δ	δ^2	pM	pN, P_1	pN, P_2	pN, P_3	pN, P'_3	pN, L_1	pN, L_2
Sun*	$1.75 \cdot 10^6$	14.8	17.5	33.3	17.5	17.5	17.5	17.5	17.5
Sun, $\psi_{\min}^{\text{Sun}} = 35^\circ$	12900	0.001	0.001	0.002	0.001	0.001	0.001	0.001	0.001
Mercury*	83.1	0.0	0.0	315	0.013	0.013	0.091	0.192	0.0
Mercury, $\psi_{\min}^{\text{Sun}} = 35^\circ$	0.007	0.0	0.0	0.0	0.0	0.0	0.0	0.0	0.0
Venus*	493	0.0	0.0	33000	0.058	0.058	0.156	0.156	0.0
Venus, $\psi_{\min}^{\text{Sun}} = 35^\circ$	493	0.0	0.0	33300	0.058	0.058	0.145	0.144	0.0
Earth*	574	0.0	0.0	13.8	0.0	0.0	0.0	0.0	0.0
Earth, $\psi_{\min}^{\text{Sun}} = 35^\circ$	3.85	0.0	0.0	0.0	0.0	0.0	0.0	0.0	0.0
Moon*	26.2	0.0	0.0	3.06	0.001	0.001	0.001	0.0	0.0
Moon, $\psi_{\min}^{\text{Sun}} = 35^\circ$	0.092	0.0	0.0	0.0	0.0	0.0	0.0	0.0	0.0
Mars	116	0.0	0.0	257	0.006	0.006	0.033	0.022	0.0
Jupiter	16300	0.001	0.002	21300	0.139	0.139	0.202	0.035	0.002
Saturn	5780	0.0	0.0	31300	0.020	0.020	0.035	0.008	0.0
Uranus	2080	0.0	0.0	3550	0.003	0.003	0.009	0.003	0.0
Neptune	2530	0.0	0.0	3700	0.002	0.002	0.007	0.003	0.0

Table 3. The maximal difference between the models in the simulations with circular coplanar trajectories $\mathbf{x}_A^{\text{eph}}(t)$ for the gravitating bodies. All quantities are given in μas . See caption of Table 2 and Section 3 for further details.

A.2. Post-Minkowskian approximation

Second, we use the *post-Minkowskian* properties of the metric tensor and consider all the components of $h_{\alpha\beta}$ to be of first order with respect to gravitational constant G :

$$\begin{aligned}
 h_{00} &= \mathcal{O}(G), \\
 h_{0i} &= \mathcal{O}(G), \\
 h_{ij} &= \mathcal{O}(G).
 \end{aligned} \tag{A.5}$$

No expansion in terms of c^{-1} is used here. Then, one has

$$\begin{aligned}
 \ddot{x}^i &= \frac{1}{2} c^2 h_{00,i} - h_{00,k} \dot{x}^k \dot{x}^i - \left(h_{ik,l} - \frac{1}{2} h_{kl,i} \right) \dot{x}^k \dot{x}^l - \frac{1}{2} h_{00,t} \dot{x}^i \\
 &\quad - \left(\frac{1}{c} h_{0k,j} - \frac{1}{2c^2} h_{jk,t} \right) \dot{x}^j \dot{x}^k \dot{x}^i - c (h_{0i,k} - h_{0k,i}) \dot{x}^k \\
 &\quad - h_{ik,t} \dot{x}^k - c h_{0i,t} + \mathcal{O}(G^2).
 \end{aligned} \tag{A.6}$$

The only formal difference between (A.6) and (A.4) is the last term $-c h_{0i,t}$ which has first order with respect to G , but is $\mathcal{O}(c^{-2})$ and has been omitted in (A.4). Eq. (A.6) has been derived without

body	δ	δ^2	pM	pN, P_1	pN, P_2	pN, P_3	pN, P'_3	pN, L_1	pN, L_2
------	----------	------------	------	-----------	-----------	-----------	------------	-----------	-----------

Sun	13000	0.001	0.001	0.002	0.001	0.001	0.001	0.001	0.001
Mercury	0.012	0.0	0.0	0.0	0.0	0.0	0.0	0.0	0.0
Venus	493	0.0	0.0	30000	0.058	0.058	0.147	0.149	0.0
Earth	4.75	0.0	0.0	0.001	0.0	0.0	0.0	0.0	0.0
Moon	0.125	0.0	0.0	0.0	0.0	0.0	0.0	0.0	0.0
Mars	116	0.0	0.0	385	0.008	0.008	0.040	0.025	0.0
Jupiter	16300	0.001	0.002	19600	0.175	0.175	0.255	0.038	0.002
Saturn	5780	0.0	0.0	27900	0.030	0.030	0.052	0.008	0.0
Uranus	2080	0.0	0.0	3550	0.004	0.004	0.014	0.003	0.0
Neptune	2530	0.0	0.0	3700	0.002	0.002	0.008	0.003	0.0

Table 4. The maximal difference between the models in the simulations with realistic trajectories $\mathbf{x}_A^{\text{eph}}(t)$ of the gravitating bodies taken from the JPL planetary ephemeris DE405/LE405. All quantities are given in μas . See caption of Table 2 and Section 3 for further details.

any assumption on the velocity of the bodies. This equation is valid in the first post-Minkowskian approximation which is also called weak-field limit.

A.3. Initial-value problem for the equations of motion

Initial value problem for the differential equations (A.4) and (A.6) can be formulated as

$$\mathbf{x}(t_0) = \mathbf{x}_0,$$

$$\dot{\mathbf{x}}(t_0) = c \boldsymbol{\mu} s(t_0), \quad \boldsymbol{\mu} \cdot \boldsymbol{\mu} = 1. \quad (\text{A.7})$$

Function s can be generally determined from the condition of the geodesic to be a null one:

$$g_{\alpha\beta} k^\alpha k^\beta = 0, \quad k^\alpha = \left(1, \frac{1}{c} \dot{\mathbf{x}} \right), \quad (\text{A.8})$$

which for metric (A.1) gives

$$s = \frac{\sqrt{(1 - h_{00})(1 + h_{ij}\boldsymbol{\mu}^i\boldsymbol{\mu}^j)} - h_{0i}\boldsymbol{\mu}^i}{1 + h_{ij}\boldsymbol{\mu}^i\boldsymbol{\mu}^j}. \quad (\text{A.9})$$

Note that s is a function of time and position (via the metric components $h_{\alpha\beta}$) as well as of the direction $\boldsymbol{\mu}$, but for a given trajectory of the photon it can be considered as a function of time.

Taking into account the orders of magnitude of $h_{\alpha\beta}$ given by (A.3) in the first post-Newtonian approximation one gets

$$s = 1 - \frac{1}{2}h_{00} - \frac{1}{2}h_{ij}\boldsymbol{\mu}^i\boldsymbol{\mu}^j - h_{0i}\boldsymbol{\mu}^i + \mathcal{O}(c^{-4}). \quad (\text{A.10})$$

It is easy to see that this expression is valid also in the first post-Minkowskian approximation (that is, it contains all terms of (A.9) linear with respect to G).

Appendix B: Light propagation in the post-Newtonian approximation

B.1. Metric tensor

The non-Galilean components of the metric tensor in the post-Newtonian approximation read

$$\begin{aligned} h_{00} &= \frac{2}{c^2} w(t, \mathbf{x}) + O(c^{-4}), \\ h_{0i} &= -\frac{4}{c^3} w^i(t, \mathbf{x}) + O(c^{-5}), \\ h_{ij} &= \frac{2}{c^2} \delta_{ij} w(t, \mathbf{x}) + O(c^{-4}). \end{aligned} \quad (\text{B.1})$$

For moving mass monopoles the potentials has the form

$$w = \sum_A \frac{GM_A}{r_A}, \quad (\text{B.2})$$

$$w^i = \sum_A \frac{GM_A}{r_A} \dot{x}_A^i(t), \quad (\text{B.3})$$

where $r_A = |\mathbf{r}_A|$,

$$\mathbf{r}_A(t, \mathbf{x}) = \mathbf{x} - \mathbf{x}_A(t), \quad (\text{B.4})$$

$\mathbf{x}_A(t)$ is the position of body A , and $\dot{\mathbf{x}}_A(t)$ is the velocity of body A .

The metric (B.1) with potentials (B.2)–(B.3) coincide with the metric tensor in the Barycentric Celestial Reference System given by the IAU (2001) (see also Soffel et al. (2003) for a discussion). The higher-order multipole moments of the bodies' gravitational fields (B.2)–(B.3) also discussed in IAU (2001) will be ignored in this paper.

B.2. Differential equations of light propagation

The post-Newtonian equations of motion of a photon then read

$$\ddot{\mathbf{x}} = \sum_A \frac{GM_A}{r_A^2} (A_A \mathbf{n}_A + B_A \mathbf{v} + C_A \mathbf{v}_A) + O(c^{-2}), \quad (\text{B.5})$$

$$A_A = 2 + \gamma - 4\delta, \quad (\text{B.6})$$

$$B_A = 4(1 - \alpha)\delta - (1 - \beta)(2 + \gamma), \quad (\text{B.7})$$

$$C_A = -4(1 - \alpha), \quad (\text{B.8})$$

$$\alpha = 1 - \mathbf{n}_A \cdot \mathbf{v}, \quad (B.9)$$

$$\beta = 1 - \mathbf{n}_A \cdot \mathbf{v}_A, \quad (B.10)$$

$$\gamma = 1 - \mathbf{v} \cdot \mathbf{v}, \quad (B.11)$$

$$\delta = 1 - \mathbf{v} \cdot \mathbf{v}_A, \quad (B.12)$$

where $\mathbf{n}_A = \mathbf{r}_A / r_A$, $\mathbf{v} = \dot{\mathbf{x}} / c$, $\mathbf{v}_A = \dot{\mathbf{x}}_A / c$.

B.3. Initial-value problem

From the general formulas of Section A.3 the initial-value problem for (B.5)–(B.12) reads

$$\mathbf{x}(t_0) = \mathbf{x}_0,$$

$$\dot{\mathbf{x}}(t_0) = c \boldsymbol{\mu} s(t_0), \quad \boldsymbol{\mu} \cdot \boldsymbol{\mu} = 1, \quad (B.13)$$

and

$$s(t) = 1 - \frac{2}{c^2} \sum_A \frac{GM_A}{r_A(t)} (1 - 2\boldsymbol{\mu} \cdot \mathbf{v}_A(t)) + O(c^{-4}). \quad (B.14)$$

B.4. Analytical solution for a body in uniform motion

Two analytical solutions of Eqs. (B.5)–(B.12) and (B.13)–(B.14) are known: 1) the classical solution for a body at rest, i.e. $\mathbf{x}_A = \text{const}$; and 2) a solution for a body moving with a constant velocity. The first solution is clearly contained in the second one. Approximate analytical solution for bodies having a constant velocity, that is for $\mathbf{x}_A(t) = \mathbf{x}_{A0} + \mathbf{v}_A(t - t_0)$, where $\mathbf{x}_{A0} = \text{const}$ and $\mathbf{v}_A = \text{const}$ have been first derived by Klioner (1989) (see also Klioner & Kopeikin 1992). The solution reads

$$\begin{aligned} \mathbf{x}(t) &= \mathbf{x}(t_0) + c \boldsymbol{\mu} s(t_0) (t - t_0) + \Delta\mathbf{x}(t_0, t) \\ &\quad - \Delta\dot{\mathbf{x}}(t_0) (t - t_0), \end{aligned} \quad (B.15)$$

$$\frac{1}{c} \dot{\mathbf{x}}(t) = \boldsymbol{\mu} s(t_0) + \frac{1}{c} \Delta\dot{\mathbf{x}}(t) - \frac{1}{c} \Delta\dot{\mathbf{x}}(t_0), \quad (B.16)$$

$$\Delta\mathbf{x}(t_0, t) = - \sum_A \frac{2GM_A}{c^2} \left(\mathbf{d}_A \mathcal{I}_A + \mathbf{g}_A \mathcal{J}_A \right) + O(c^{-4}), \quad (B.17)$$

$$\mathbf{d}_A = \boldsymbol{\mu} \times (\mathbf{r}_{A0} \times \mathbf{g}_A), \quad (B.18)$$

$$\mathbf{g}_A = \boldsymbol{\mu} - \mathbf{v}_A, \quad (B.19)$$

$$\mathcal{I}_A = \frac{1}{|\mathbf{g}_A| |\mathbf{r}_A| - \mathbf{g}_A \cdot \mathbf{r}_A} - \frac{1}{|\mathbf{g}_A| |\mathbf{r}_{A0}| - \mathbf{g}_A \cdot \mathbf{r}_{A0}}, \quad (B.20)$$

$$\mathcal{J}_A = \log \frac{|\mathbf{g}_A| |\mathbf{r}_A| + \mathbf{g}_A \cdot \mathbf{r}_A}{|\mathbf{g}_A| |\mathbf{r}_{A0}| + \mathbf{g}_A \cdot \mathbf{r}_{A0}}, \quad (B.21)$$

$$\mathbf{r}_A(t) = \mathbf{x}(t) - \mathbf{x}_A(t), \quad (B.22)$$

$$\mathbf{r}_{A0} = \mathbf{x}(t_0) - \mathbf{x}_A(t_0), \quad (\text{B.23})$$

$$\frac{1}{c} \Delta \dot{\mathbf{x}}(t) = - \sum_A \frac{2GM_A}{c^2} \left(\mathbf{d}_A \frac{1}{c} \dot{\mathcal{I}}_A + \mathbf{g}_A \frac{1}{c} \dot{\mathcal{J}}_A \right) + O(c^{-4}), \quad (\text{B.24})$$

$$\frac{1}{c} \dot{\mathcal{I}}_A = \frac{|\mathbf{g}_A|}{|\mathbf{r}_A| (|\mathbf{g}_A| |\mathbf{r}_A| - \mathbf{g}_A \cdot \mathbf{r}_A)}, \quad (\text{B.25})$$

$$\frac{1}{c} \dot{\mathcal{J}}_A = \frac{|\mathbf{g}_A|}{|\mathbf{r}_A|}. \quad (\text{B.26})$$

This solution has two parameters \mathbf{x}_{A0} and \mathbf{v}_A . Note that the values of \mathbf{x}_{A0} and \mathbf{v}_A are arbitrary and it is apriori unclear how to relate \mathbf{x}_{A0} to the actual trajectory $\mathbf{x}_A^{\text{eph}}(t)$ of the body in order to minimize the errors (see Section 3).

The classical solution of (B.5)–(B.12) for a body at rest can be easily restored from (B.15)–(B.26) by setting $\mathbf{v}_A = 0$ that implies $\mathbf{g}_A = \mu$ and $|\mathbf{g}_A| = 1$.

Appendix C: Theoretical results in the post-Minkowskian approximation

C.1. Metric tensor

In the post-Minkowskian approximation the metric tensor of a system of arbitrarily moving mass monopole can be written (see Kopeikin & Schäfer (1999); Kopeikin & Mashhoon (2002)) with retarded potentials similar to the Lienard-Wiechert potentials which are well known from the classical electrodynamics (Jackson 1974). The metric reads

$$\begin{aligned} h_{00} &= \frac{2}{c^2} \mathcal{W}(t, \mathbf{x}) + O(G^2), \\ h_{0i} &= -\frac{4}{c^3} \mathcal{W}^i(t, \mathbf{x}) + O(G^2), \\ h_{ij} &= \frac{2}{c^2} \mathcal{W}^{ij}(t, \mathbf{x}) + O(G^2), \end{aligned} \quad (\text{C.1})$$

$$\mathcal{W}(t, \mathbf{x}) = \sum_A \frac{GM_A}{r_A^* \beta_*} \left(2\Gamma_* - \Gamma_*^{-1} \right), \quad (\text{C.2})$$

$$\mathcal{W}^i(t, \mathbf{x}) = \sum_A \frac{GM_A}{r_A^* \beta_*} \Gamma_* c v_A^{*i}, \quad (\text{C.3})$$

$$\mathcal{W}^{ij}(t, \mathbf{x}) = \sum_A \frac{GM_A}{r_A^* \beta_*} \left(\delta^{ij} \Gamma_*^{-1} + 2\Gamma_* v_A^{*i} v_A^{*j} \right), \quad (\text{C.4})$$

where $\mathbf{r}_A^* = \mathbf{x} - \mathbf{x}_A^*$, $r_A^* = |\mathbf{r}_A^*|$, $\mathbf{x}_A^* = \mathbf{x}_A(t_A^*)$, $\mathbf{v}_A^* = \frac{d}{dt_A^*} \mathbf{x}_A^*/c$, $\mathbf{n}_A^* = \mathbf{r}_A^*/r_A^*$, $\beta_* = 1 - \mathbf{n}_A^* \cdot \mathbf{v}_A^*$, $\Gamma_* = (1 - \mathbf{v}_A^* \cdot \mathbf{v}_A^*)^{-1/2}$. Here and below in Section C the position \mathbf{x}_A , velocity $\dot{\mathbf{x}}_A$ and acceleration $\ddot{\mathbf{x}}_A$ of the gravitating bodies are computed at the time moment $t_A^* = t_A^*(t, \mathbf{x})$ being the retarded moment of time defined by the following implicit equation

$$t_A^* + \frac{1}{c} r_A^* = t. \quad (\text{C.5})$$

Note that $r_A(t) = r_A^* \beta_* + O(r_A^2/c^2)$, so that formally $\mathcal{W} = w + O(c^{-2})$, $\mathcal{W}^i = w^i + O(c^{-2})$, $\mathcal{W}^{ij} = \delta^{ij} w + O(c^{-2})$, and Eqs. (B.1)–(B.4) can be easily restored from (C.1)–(C.4) within the first post-Newtonian approximation.

C.2. Differential equations of light propagation

Substituting (C.1) into (A.6) one gets

$$\ddot{\mathbf{x}} = \mathcal{W}_{,i} - \frac{2}{c^2} \mathcal{W}_{,k} \dot{x}^k \dot{x}^i - \frac{2}{c^2} \mathcal{W}^{ik}_{,l} \dot{x}^k \dot{x}^l + \frac{1}{c^2} \mathcal{W}^{kl}_{,i} \dot{x}^k \dot{x}^l - \frac{1}{c^2} \mathcal{W}_{,t} \dot{x}^i + \frac{4}{c^4} \mathcal{W}^k_{,j} \dot{x}^j \dot{x}^k \dot{x}^i + \frac{1}{c^4} \mathcal{W}^{jk}_{,t} \dot{x}^j \dot{x}^k \dot{x}^i + \frac{4}{c^2} \mathcal{W}^i_{,k} \dot{x}^k - \frac{4}{c^2} \mathcal{W}^k_{,i} \dot{x}^k - \frac{2}{c^2} \mathcal{W}^{ik}_{,t} \dot{x}^k + \frac{4}{c^2} \mathcal{W}^i_{,t} + O(G^2). \quad (\text{C.6})$$

Here, as usual, $A_{,t} = \frac{\partial}{\partial t} A$ is the partial derivative with respect to t , and for any latin index i with $i \neq t$ one has $A_{,i} = \frac{\partial}{\partial x^i} A$. Since the potentials \mathcal{W} , \mathcal{W}^i and \mathcal{W}^{ij} are given by Eqs. (C.2)–(C.4) explicitly as functions of the retarded time $t_A^* = t_A^*(t, \mathbf{x})$ one has to use

$$\frac{\partial}{\partial t} A(t, \mathbf{x}) = \frac{\partial A(t_A^*, \mathbf{x})}{\partial t_A^*} \frac{\partial t_A^*}{\partial t}, \quad (\text{C.7})$$

$$\frac{\partial}{\partial x^i} A(t, \mathbf{x}) = \frac{\partial A(t_A^*, \mathbf{x})}{\partial t_A^*} \frac{\partial t_A^*}{\partial x^i} + \frac{\partial A(t_A^*, \mathbf{x})}{\partial x^i}, \quad (\text{C.8})$$

where from (C.5)

$$\frac{\partial t_A^*}{\partial t} = \beta_*^{-1}, \quad (\text{C.9})$$

$$\frac{\partial t_A^*}{\partial x^i} = -c^{-1} \beta_*^{-1} n_A^{*i}. \quad (\text{C.10})$$

Substituting (C.2)–(C.4) into (C.6) and using (C.7)–(C.8) one gets the explicit form of the equations of motion of a photon in the first post-Minkowskian approximation

$$\ddot{\mathbf{x}} = \sum_A \frac{GM_A \Gamma_*^3}{r_A^{*2} \beta_*^3} (\mathcal{A}_A \mathbf{n}_A^* + \mathcal{B}_A \mathbf{v} + \mathcal{C}_A \mathbf{v}_A^* + \mathcal{D}_A \mathbf{a}_A^*) + O(G^2), \quad (\text{C.11})$$

$$\mathcal{A}_A = \left[\Gamma_*^{-2} \gamma - 2 \delta_*^2 \right] \Gamma_*^{-2} \left(\Gamma_*^{-2} + \varepsilon_* \right) - \left[\Gamma_*^{-2} \gamma + 2 \delta_*^2 \right] \eta_* \beta_* + 4 \zeta_* \Gamma_*^{-2} \beta_* \delta_*, \quad (\text{C.12})$$

$$\begin{aligned} \mathcal{B}_A = \Gamma_*^{-2} & \left[-\Gamma_*^{-4} \gamma - \Gamma_*^{-2} \left\{ 2\delta_*(2\alpha_* - \delta_*) + (\epsilon_* - \beta_*) \gamma \right\} \right. \\ & \left. + 2\delta_* \{\beta_* \delta_* - \epsilon_* (2\alpha_* - \delta_*)\} + 4\zeta_* \beta_* (\alpha_* - \delta_*) \right] \\ & + \eta_* \beta_* \left(\Gamma_*^{-2} \gamma - 2\delta_*(2\alpha_* - \delta_*) \right), \end{aligned} \quad (\text{C.13})$$

$$\mathcal{C}_A = \Gamma_*^{-4} [4 \delta_* \alpha_* - \beta_* \gamma]$$

$$+2\Gamma_*^{-2} \left[\delta_* \{ 2\epsilon_* \alpha_* - \beta_* \delta_* \} - 2\zeta_* \beta_* \alpha_* \right] \\ +4\eta_* \alpha_* \beta_* \delta_*, \quad (C.14)$$

$$\mathcal{D}_A = 4\Gamma_*^{-2} \alpha_* \beta_* \delta_* c^{-1} r_A^*, \quad (C.15)$$

$$\alpha_* = 1 - \mathbf{n}_A^* \cdot \mathbf{v}, \quad (C.16)$$

$$\beta_* = 1 - \mathbf{n}_A^* \cdot \mathbf{v}_A^*, \quad (C.17)$$

$$\gamma = 1 - \mathbf{v} \cdot \mathbf{v}, \quad (C.18)$$

$$\delta_* = 1 - \mathbf{v} \cdot \mathbf{v}_A^*, \quad (C.19)$$

$$\epsilon_* = (\mathbf{a}_A^* \cdot \mathbf{n}_A^*) c^{-1} r_A^*, \quad (C.20)$$

$$\zeta_* = (\mathbf{a}_A^* \cdot \mathbf{v}) c^{-1} r_A^*, \quad (C.21)$$

$$\eta_* = (\mathbf{a}_A^* \cdot \mathbf{v}_A^*) c^{-1} r_A^*, \quad (C.22)$$

$$\text{and } \mathbf{v} = c^{-1} \frac{d}{dt} \mathbf{x}, \mathbf{a}_A^* = \frac{d}{dt} \mathbf{v}_A^* = c^{-1} \frac{d^2}{dt^2} \mathbf{x}_A(t_A^*).$$

From Eqs. (C.11)–(C.22) one can restore the post-Newtonian equations of motion (B.5)–(B.12) neglecting in (C.11)–(C.22) all the terms formally of order $O(c^{-2})$ (e.g., all the acceleration-dependent terms) and taking into account that in (C.11)–(C.22) the position of the bodies are calculated at the retarded moment of time t_A^* while in (B.5)–(B.12) at moment t . The latter circumstance gives the following relations: $\mathbf{r}_A(t) = \mathbf{r}_A^* - \mathbf{r}_A^* \mathbf{v}_A^* + O(c^{-2})$, $r_A(t) = r_A^* \beta_* + O(c^{-2})$, $\mathbf{n}(t) = (\mathbf{n}_A^* - \mathbf{v}_A^*)/\beta_* + O(c^{-2})$.

Since from (C.11) it follows that

$$\mathbf{x} = \mathbf{x}_0 + c \boldsymbol{\mu} (t - t_0) + O(G), \quad \boldsymbol{\mu} \cdot \boldsymbol{\mu} = 1 \quad (C.23)$$

in the first post-Minkowski approximation in the right-hand side of Eq. (C.11) one can put

$$\mathbf{x} = \mathbf{x}_0 + c \boldsymbol{\mu} (t - t_0), \quad \boldsymbol{\mu} \cdot \boldsymbol{\mu} = 1 \quad (C.24)$$

and, therefore, $\mathbf{v} = \boldsymbol{\mu}$, which implies, e.g., $\gamma = 0$. Formally, this makes Eq. (C.11) integrable in quadratures (since the right-hand side is simply a function of time). We prefer here not to do so and retain Eq. (C.11) in the form of a differential equation as given by (C.6).

C.3. Initial-value problem

Initial value problem for Eq. (C.11)

$$\mathbf{x}(t_0) = \mathbf{x}_0,$$

$$\dot{\mathbf{x}}(t_0) = c \boldsymbol{\mu} \tilde{s}(t_0), \quad \boldsymbol{\mu} \cdot \boldsymbol{\mu} = 1 \quad (C.25)$$

with

$$\tilde{s}(t) = 1 - \frac{2}{c^2} \sum_A \frac{GM_A \Gamma_*}{r_A^* \beta_*} \theta_*^2 + O(G^2), \quad (\text{C.26})$$

$$\theta_* = 1 - \boldsymbol{\mu} \cdot \boldsymbol{v}_A^*. \quad (\text{C.27})$$

C.4. Analytical solution in the post-Minkowskian approximation

The explicit form of the analytical solution in the first post-Minkowskian approximation derived by Kopeikin & Schäfer (1999) reads

$$\begin{aligned} \mathbf{x}(t) = & \mathbf{x}(t_0) + c \boldsymbol{\mu} \tilde{s}(t_0) (t - t_0) + \tilde{\Delta}\mathbf{x}(t_0, t) \\ & - \tilde{\Delta}\dot{\mathbf{x}}(t_0) (t - t_0), \end{aligned} \quad (\text{C.28})$$

$$\frac{1}{c} \dot{\mathbf{x}}(t) = \boldsymbol{\mu} \tilde{s}(t_0) + \frac{1}{c} \tilde{\Delta}\dot{\mathbf{x}}(t) - \frac{1}{c} \tilde{\Delta}\dot{\mathbf{x}}(t_0), \quad (\text{C.29})$$

$$\tilde{\Delta}\mathbf{x}(t_0, t) = - \sum_A \frac{2GM_A}{c^2} \left(\mathbf{f}(t) - \mathbf{f}(t_0) + \mathbf{g}(t_0, t) \right) + O(G^2), \quad (\text{C.30})$$

$$\mathbf{f}(t) = \Gamma_* \left(\theta_* \frac{\boldsymbol{\mu} \times (\mathbf{r}_A^* \times \boldsymbol{\mu})}{r_A^* \alpha_*} - (\boldsymbol{\mu} - \boldsymbol{v}_A^*) \log(r_A^* \alpha_*) \right), \quad (\text{C.31})$$

$$\begin{aligned} \mathbf{g}(t_0, t) = & \int_{t_0}^t \frac{\Gamma_*^3}{r_A^* \beta_*} \left[\left(\Gamma_*^2 \zeta_* - \theta_* \eta_* \right) \boldsymbol{\mu} \times (\mathbf{n}_A^* \times \boldsymbol{\mu}) \right. \\ & \left. + \alpha_* \log(r_A^* \alpha_*) \left(\eta_* (\boldsymbol{\mu} - \boldsymbol{v}_A^*) - \Gamma_*^{-2} c^{-1} r_A^* \boldsymbol{a}_A^* \right) \right] c dt, \end{aligned} \quad (\text{C.32})$$

$$\begin{aligned} \frac{1}{c} \tilde{\Delta}\dot{\mathbf{x}}(t) = & - \sum_A \frac{2GM_A}{c^2} \frac{\Gamma_* \theta_*}{r_A^* \beta_*} \left(\theta_* \frac{\boldsymbol{\mu} \times (\mathbf{n}_A^* \times \boldsymbol{\mu})}{\alpha_*} \right. \\ & \left. + (2 - \theta_*) \boldsymbol{\mu} - 2 \boldsymbol{v}_A^* \right) + O(G^2). \end{aligned} \quad (\text{C.33})$$

Here $\mathbf{g}(t_0, t)$ are integrals depending on the accelerations of the bodies. The integrals can be transformed into integrals with respect to retarded time s as described in Kopeikin & Schäfer (1999). In the right-hand sides of (C.30) and (C.33) one should put $\mathbf{x}(t) = \mathbf{x}(t_0) + c \boldsymbol{\mu} (t - t_0)$.

Note that the solution for $\frac{1}{c} \tilde{\Delta}\dot{\mathbf{x}}(t)$ is exact within the first post-Minkowskian approximation (i.e. all the omitted terms are of order G^2). It is remarkable that this solution can be written in such a compact closed form for arbitrary motion of the gravitating bodies. Note also that the solution depends only on the position and velocity of the bodies in a single moment of time – the retarded moment corresponding to time t – and does not depend on the previous motion of the bodies. If all the terms which are formally of order $O(c^{-4})$ (these are the terms at least quadratic with respect to \boldsymbol{v}_A) are dropped both in (C.33) and (B.24) the two formulas are equivalent. One can also show that Eqs. (C.30)–(C.31) agree with Eqs. (B.17)–(B.21) in the first post-Newtonian approximation provided that \boldsymbol{v}_A is considered to be constant.

Taking into account that for any function A^i and $\mathbf{x}(t) = \mathbf{x}_0 + c \boldsymbol{\mu} (t - t_0)$

$$\begin{aligned} \frac{d}{dt} A^i(t, \mathbf{x}(t)) &= \frac{\partial}{\partial t} A^i(t, \mathbf{x}(t)) + \frac{\partial}{\partial x^j} A^i(t, \mathbf{x}(t)) c \mu^j \\ &= \frac{\alpha_*}{\beta_*} \frac{\partial}{\partial t^*} A^i(t^*, \mathbf{x}(t)) + \frac{\partial}{\partial x^j} A^i(t^*, \mathbf{x}(t)) c \mu^j, \end{aligned} \quad (\text{C.34})$$

one can prove that a time derivative of (C.33) exactly coincides with the post-Minkowskian equations of motion for a photon (C.11)–(C.22) provided that v is taken to be equal to μ in the latter (this is allowed within the first post-Minkowskian approximation as discussed above).

A different way to derive the Kopeikin-Schäfer solution (C.28)–(C.33) for the case of bodies moving with constant velocities is given by Klioner (2003b) who has shown how to derive this solution combining the post-Newtonian solution (B.15)–(B.26) for a motionless body ($v_A = 0$) with a suitable Lorentz transformation.

Appendix D: Two point boundary value problem for the analytical solutions

Let us consider analytical equations of light propagation in the form valid for both analytical models discussed above

$$\begin{aligned} \mathbf{x}(t) &= \mathbf{x}(t_0) + c \mu s(t_0) (t - t_0) + \Delta \mathbf{x}(t_0, t) \\ &\quad - \Delta \dot{\mathbf{x}}(t_0) (t - t_0) + \mathcal{O}(\epsilon^2), \end{aligned} \quad (\text{D.1})$$

$$\frac{1}{c} \dot{\mathbf{x}}(t) = \mu s(t_0) + \frac{1}{c} \Delta \dot{\mathbf{x}}(t) - \frac{1}{c} \Delta \dot{\mathbf{x}}(t_0) + \mathcal{O}(\epsilon^2), \quad (\text{D.2})$$

with

$$\Delta \mathbf{x}(t_0, t_0) = 0, \quad (\text{D.3})$$

$$\lim_{t \rightarrow -\infty} \frac{1}{c} \Delta \dot{\mathbf{x}}(t) = 0. \quad (\text{D.4})$$

These two conditions can be proven to be valid for both analytical models considered above. The small parameter ϵ can be identified with G for the post-Minkowskian solution and with c^{-2} for the post-Newtonian solution, so that in both solutions $\Delta \mathbf{x}(t_0, t) = \mathcal{O}(\epsilon)$ and $c^{-1} \Delta \dot{\mathbf{x}}(t) = \mathcal{O}(\epsilon)$.

Let us define several vectors

$$\boldsymbol{\sigma} = \lim_{t \rightarrow -\infty} \frac{1}{c} \dot{\mathbf{x}}(t), \quad (\text{D.5})$$

$$\mathbf{n} = \mathbf{n}(t) = \frac{\dot{\mathbf{x}}(t)}{|\dot{\mathbf{x}}(t)|}, \quad (\text{D.6})$$

$$\mathbf{k} = \mathbf{k}(t_0, t) = \frac{\mathbf{R}(t_0, t)}{|\mathbf{R}(t_0, t)|}, \quad (\text{D.7})$$

$$\mathbf{R} = \mathbf{R}(t_0, t) = \mathbf{x}(t) - \mathbf{x}(t_0). \quad (\text{D.8})$$

These definitions are illustrated on Figure 2. Vector $\boldsymbol{\sigma}$ is the unit direction of the light path at past null infinity ($t \rightarrow -\infty$). Vector $\mathbf{n}(t)$ is the unit direction of light propagation at time moment

t (so that $\mathbf{n}(t_0) = \boldsymbol{\mu}$ and $\lim_{t \rightarrow -\infty} \mathbf{n}(t) = \boldsymbol{\sigma}$). Vector \mathbf{k} is the unit vector connecting the points $\mathbf{x}(t_0)$ and $\mathbf{x}(t)$. Now, if one considers the points $\mathbf{x}(t_0)$ and $\mathbf{x}(t)$ as given constants, one gets from (D.1)–(D.4) the following formulas approximately solving the two point boundary value problem for the differential equations of motion

$$\boldsymbol{\sigma} = \boldsymbol{\mu} - \boldsymbol{\mu} \times \left(\frac{1}{c} \Delta \dot{\mathbf{x}}(t_0) \times \boldsymbol{\mu} \right) + O(\epsilon^2), \quad (\text{D.9})$$

$$s(t) = 1 + \frac{1}{c} \boldsymbol{\mu} \cdot \Delta \dot{\mathbf{x}}(t) + O(\epsilon^2), \quad (\text{D.10})$$

$$\mathbf{n} = \boldsymbol{\mu} + \boldsymbol{\mu} \times \left(\left[\frac{1}{c} \Delta \dot{\mathbf{x}}(t) - \frac{1}{c} \Delta \dot{\mathbf{x}}(t_0) \right] \times \boldsymbol{\mu} \right) + O(\epsilon^2), \quad (\text{D.11})$$

$$\mathbf{k} = \boldsymbol{\mu} + \boldsymbol{\mu} \times \left(\left[-\frac{1}{c} \Delta \dot{\mathbf{x}}(t_0) + \frac{1}{|\mathbf{R}|} \Delta \mathbf{x}(t_0, t) \right] \times \boldsymbol{\mu} \right) + O(\epsilon^2), \quad (\text{D.12})$$

$$\mathbf{n} = \mathbf{k} + \mathbf{k} \times \left(\left[\frac{1}{c} \Delta \dot{\mathbf{x}}(t) - \frac{1}{|\mathbf{R}|} \Delta \mathbf{x}(t_0, t) \right] \times \mathbf{k} \right) + O(\epsilon^2). \quad (\text{D.13})$$

Note that (D.9) follows from (D.11) for $t \rightarrow -\infty$, that (D.13) is a combination of (D.11) and (D.12), and that (D.10) agrees with the expressions (B.14) and (C.26) for $s(t)$ given above for the post-Newtonian and the post-Minkowskian solutions, respectively. From (D.12) and the corresponding expressions for $\dot{\mathbf{x}}(t)$ and $\Delta \mathbf{x}(t_0, t)$ one can see that for a given impact parameter of the light ray the difference between vectors \mathbf{k} and $\boldsymbol{\mu}$ becomes smaller for greater distances between the gravitating body and point of emission $\mathbf{x}(t_0)$.

Note that $\Delta \mathbf{x}(t_0, t)$, $\Delta \dot{\mathbf{x}}(t)$ and $\Delta \dot{\mathbf{x}}(t_0)$ on the right-hand sides of (D.9)–(D.13) depend on $\boldsymbol{\mu}$. Formally, considering only analytical orders of magnitude one could replace $\boldsymbol{\mu}$ by \mathbf{k} in these formulas. However, this works well only when the impact parameters computing for the unperturbed trajectories with directions $\boldsymbol{\mu}$ and \mathbf{k} are sufficiently close to one another. This is not always the case. For example, this assumption is wrong in the gravitational lens limit. It is more safe to calculate vector $\boldsymbol{\mu}$ from given \mathbf{k} by a numerical inversion of (D.12) and then calculate \mathbf{n} from (D.11) or (D.13).

References

Bienaymé, O. & Turon, C. eds. 2002, GAIA: A European Space Project (Les Ulis: EDP Sciences)

Brumberg, V.A. 1991, Essential Relativistic Celestial Mechanics (Bristol: Hilger)

Brumberg, V.A., Klioner, S.A., & Kopejkin, S.M. 1990, in Inertial Coordinate System on the Sky, ed. J.H. Lieske & V.K. Abalakin (Dordrecht: Kluwer), 229

Char, B.W., Geddes, K.O., Gonnet, G.H. et al. 1993, MAPLE V Library Reference Manual, (New York: Springer)

de Felice, F., Bucciarelli, B., Lattanzi, M.G., & Vecchiato, A. 2001, A&A, 373, 336

de Felice, F., Lattanzi, M.G., Vecchiato, A., & Bernacca, P.L. 1998, A&A, 332, 1133

de Felice, F., Vecchiato, A., Bucciarelli, B., Lattanzi, M.G., & Crosta, M. 2000, in Towards Models and Constants for Sub-Microarcsecond Astrometry, ed. K.J. Johnston, D.D. McCarthy, B.J. Luzum, & G.H. Kaplan (Washington: US Naval Observatory), 314

ESA. 2000 GAIA: Composition, Formation and Evolution of the Galaxy, Concept and Technology Study Report (ESA-SCI[2000]4) (Noordwijk: ESA)

Everhart, E. 1974, Celestial Mechanics, 10, 35

Everhart, E. 1985, in Dynamics of Comets: Their Origin and Evolution, ed. A. Carusi & G.B. Valsecchi, Astrophysics and Space Science Library, **115** (Dordrecht: Reidel), 185

Hellings, R.W. 1986, AJ, 91, 650

IAU 2001, Information Bulletin, 88 (errata in IAU Information Bulletin, 89)

Jackson, J. D. 1974, Classical Electrodynamics (New York: Wiley)

Klioner, S. A. 1989, Soobschch. Inst. Prikl. Astron. No 6 (Communications of the Institute of Applied Astronomy, No 6, St. Petersburg, in Russian)

Klioner, S. A. 1991, in: Geodetic VLBI: Monitoring Global Change, ed. W.E. Carter, NOAA Technical Report NOS 137 NGS 49, 188 (Washington D.C.: American Geophysical Union)

Klioner, S. A. 2003a, AJ, 125, 1580

Klioner, S. A. 2003b, Light Propagation in the Gravitational Field of Moving Bodies by means of Lorentz Transformation I. Mass monopoles moving with constant velocities A&A, in press (preprint available as <http://arxiv.org/abs/astro-ph/0301573>)

Klioner, S. A., Kopeikin, S. M. 1992, AJ, 104, 897

Kopeikin, S. M. 1997, J. Math. Phys., 38, 2587

Kopeikin, S. M., Schäfer, G. 1999, Phys. Rev. D, 60, No. 124002

Kopeikin, S. M., Mashhoon, B. 2002, Phys. Rev. D, 65, No. 64025

Mignard, F. 2002, Considerations on the orbit of GAIA for simulations, GAIA-FM-011

Perryman, M.A.C., et al., 2001, A&A, 369, 339

Shao, M., 1998, Proc. SPIE, 3350, 536

Soffel, M., Klioner S.A., Petit, G. et al. 2003, The IAU 2000 resolutions for astrometry, celestial mechanics and metrology in the relativistic framework: explanatory supplement, AJ, in press

Weissman, P.R., McFadden, L.-A., Johnson, T.V. (eds.) 1999, Encyclopedia of the Solar System (San Diego: Academic Press)

Will, C. M. 1993, Theory and experiment in gravitational physics (rev. ed.; Cambridge: Cambridge University Press)